

weak-coupling case this coincides more or less with the kinematical line position of the line in question, however in the case of strong coupling, a line g will split into two branches and each of these may be considerably displaced from the kinematical two-beam position near the three- (many-) beam condition (Høier, Zuo, Marthinsen & Spence, 1988). The largest differences between cases of opposite signs of the triplet phase seems to be for the former case where the two cases have a clear maximum or minimum near the kinematical three-beam condition. However, in the strong-coupling case relatively large quantitative differences may also be observed but the magnitude of the differences and thus the possibility to distinguish cases of opposite triplet phases is strongly dependent on the thickness.

However, it is difficult to find any simple rule as to which thicknesses give the largest differences. This is because the intensity difference in general is the result of the difference between several thickness-dependent terms in the intensity expression [(10)], each depending on the magnitude of a product of eigenvector components and a cosine term for which the argument is a sum of a t -dependent term and the phase of the product of eigenvector components in the prefactor. It is impossible to draw any general conclusions about which thicknesses maximize this complicated difference term.

In general, the determination of the correct sign of a triplet phase has to be based on high-quality experiments and quantitative intensity recordings. To avoid thickness averaging, which may blur the intensity variations of interest, CBED patterns should be obtained from parallel-sided specimens or the area from which the patterns are obtained should be so small that possible thickness variations are negligible.

Experiments should further be carried out at liquid-nitrogen temperature using a cooling holder to minimize thermal diffuse scattering. Finally, quantitative comparisons should preferentially be based on digitized energy-filtered intensity data. Instrumentation for acquiring intensity data in this latter way are now under development and the use of such systems will increase the potential for quantitative CBED considerably in the future (see, for example, Spence, Mayer & Zuo, 1991; Marthinsen, Runde, Holmestad & Høier, 1991).

References

- BETHE, H. (1928). *Ann. Phys. (Leipzig)*, **87**, 55–129.
 BIRD, D. M., JAMES, R. & PRESTON, A. R. (1987). *Phys. Rev. Lett.* **59**, 1216–1219.
 BUXTON, B. F., EADES, J. A., STEEDS, J. W. & RACKHAM, G. M. (1976). *Philos. Trans. R. Soc. London Ser. A*, **281**, 171–194.
 GJØNNES, J. & HØIER, R. (1971). *Acta Cryst.* **A27**, 313–316.
 HØIER, R., ZUO, J. M., MARTHINSEN, K. & SPENCE, J. C. H. (1988). *Ultramicroscopy*, **26**, 25–30.
 HUMPHREYS, C. J. (1979). *Rep. Prog. Phys.* **42**, 1825–1887.
 KAMBE, K. (1957). *J. Phys. Soc. Jpn*, **12**, 1–13.
 MARTHINSEN, K. (1991). Report STF19 A91039. SINTEF, Trondheim, Norway.
 MARTHINSEN, K. & HØIER, R. (1988). *Acta Cryst.* **A44**, 558–562.
 MARTHINSEN, K. & HØIER, R. (1989). *Proc. 47th Annu. Meet. Electron Microsc. Soc. Am.*, edited by G. W. BAILY, pp. 484–485. San Francisco Press.
 MARTHINSEN, K., RUNDE, P., HOLMESTAD, R. & HØIER, R. (1991). *Electron Microscopy and Analysis 1991. Inst. Phys. Conf. Series* No. 119, edited by F. J. HUMPHREYS, pp. 367–370. Bristol: Institute of Physics.
 SPENCE, J. C. H., MAYER, J. & ZUO, J. M. (1991). *Micron Microsc. Acta*, **22**, 173–174.
 ZUO, J. M., GJØNNES, K. & SPENCE, J. C. H. (1989). *J. Electron Microsc. Tech.* **12**, 29–55.
 ZUO, J. M., HØIER, R. & SPENCE, J. C. H. (1989). *Acta Cryst.* **A45**, 839–851.

Acta Cryst. (1993). **A49**, 330–335

On the X-ray Reflectivity of Absorbing Crystals

BY P. D. MORAN

Materials Science Program, University of Wisconsin, Madison, WI 53706, USA

AND R. J. MATYI

Department of Materials Science and Engineering, University of Wisconsin, Madison, WI 53706, USA

(Received 28 January 1992; accepted 21 August 1992)

Abstract

A simple relationship is reported defining the ratio of dynamical and kinematic values of the integrated reflectivity in absorbing single crystals in terms of the

product $\mu_n \xi$, where μ_n is the linear absorption coefficient for depth measured along the normal to the diffracting crystal's surface and ξ is the extinction distance in a nonabsorbing crystal. This relationship is interpreted through comparison with existing

(albeit mathematically complicated) expressions for the dynamical reflectivity in the two limits of negligible absorption and very strong absorption. It is shown to be valid for intermediate values of $\mu_n \xi$ by comparison with calculated values of the integrated reflection from single-crystal CdTe using various wavelengths and $\langle 111 \rangle$ -type reflections. This relationship's usefulness is discussed in the analysis of dynamical diffraction experiments commonly employed in semiconductor materials characterization.

Introduction

It is well known that the integrated intensity of a Bragg reflection from a highly perfect crystal can differ considerably from that recorded from a structurally imperfect crystal of the same material. The diffraction process in imperfect crystals is described by the kinematic theory, whereas diffraction from perfect crystals is best described by the dynamical theory. The well defined difference in the value of the integrated reflection for perfect and imperfect crystals immediately suggests the utility of measuring this quantity as a nondestructive gauge of crystalline perfection (White, 1950). In the kinematic theory, it is assumed that the crystal is not structurally perfect over a distance sufficient to provide a coherent medium where the diffracted and incident X-ray wavefronts can dynamically couple with each other. The resulting expression for the integrated reflectivity for X-rays with wavelength λ diffracting from a material with unit-cell volume V_c at the Bragg angle θ_B is given as (James, 1963)

$$R_{\text{kin}} = (\pi^2 |\Phi_h|^2 / 2\lambda\mu \sin 2\theta_B) C^2 \quad (1)$$

with

$$\Phi_h = (r_e \lambda^2 / \pi V_c) F_h, \quad (2)$$

where r_e is the classical electron radius, μ is the photoelectron absorption coefficient, $F_h = F_{hkl}$ is the structure factor, C is the polarization factor and Φ_h denotes the hkl Fourier component of the electric susceptibility expanded over the crystal's reciprocal lattice. Note that in the above equation, as in all that will follow, the symmetric Bragg diffraction geometry is assumed so that the diffracting planes are considered parallel to the crystal surface. Generalization from the symmetric case is straightforward, involving the multiplication of parameters by an average of the sines of the angles incident and diffracted X-rays make with the surface (see, for instance, Afanas'ev & Perstnev, 1969; James, 1963).

The dynamical theory of diffraction is invoked to describe the perfect-crystal case. In this theory, the effect of the periodic medium on the coupling of incident and diffracted X-rays is taken into consider-

ation. The incident and diffracted wave fronts are considered as parts of a wave field existing in the crystal that interact with each other and the periodically varying electrical susceptibility of the medium in such a way as to satisfy Maxwell's equations within the crystal. The resulting expression for integrated reflectivity has two forms depending on whether or not the absorption of the crystal is considered to be of appreciable magnitude. If one can neglect absorption, the dynamical expression for the integrated Bragg reflection corresponding to (1) is given by James (1963) as

$$R_{\text{dyn}} = (8 |\Phi_h| / 3 \sin 2\theta_B) C. \quad (3)$$

When absorption cannot be neglected, the simple expression (3) is no longer valid. The first theoretically rigorous analytic expression for the integrated reflectivity from a crystal in which no assumptions were made about the magnitude of absorption was derived by Afanas'ev & Perstnev (1969). Earlier, an empirical relationship developed by Hirsch & Ramachandran (1949) was used quite successfully to describe the reflectivity of the absorbing perfect crystal. Although Hirsch & Ramachandran (1949) considered only centrosymmetric structures, a generalization of the expression by Cole & Stemple (1962) encompassing noncentrosymmetric crystals is

$$R_{\text{dyn}} = (|C\Phi_{hr}| / \sin 2\theta_B) [(\pi/4)(1 + \kappa^2 + 2s) / |g| + \exp\{-(1 - \kappa^2)^2 + 4p^2\} \times [|g| + \ln(32/3\pi)]] \quad (4)$$

where

$$g = |\Phi_{oi}| / |C| |\Phi_{hr}|, \quad k = |\Phi_{hi}| / |\Phi_{hr}|, \\ p = [\text{Re}(\Phi_{hr}) \text{Re}(\Phi_{hi}) + \text{Im}(\Phi_{hr}) \text{Im}(\Phi_{hi})] / |\Phi_{hr}|^2. \quad (5)$$

Note that the r and i in Φ_{hr} or Φ_{hi} reference whether the quantity is derived from summing the real or imaginary components of the atomic structure factors over the unit cell. Again, the above expression, though accurate, is empirical in nature. The relationship was developed by studying numerical integrations of calculated reflection profiles. The rigorous analytic expression for the integrated reflection derived by Afanas'ev & Perstnev (1969) is

$$R_{\text{dyn}} = (8/3 \sin 2\theta_B) |C\Phi_h| (|\Phi_h| / |\Phi_h|)^{1/2} P(s, q), \quad (6)$$

where

$$P(s, q) = (1 - s^2 - 2q^2 s^2) E(k) / k \\ - (3\pi/4) s(1 - 2q^2 s^2) \\ + ks^2(1 - q^2) [3(1 - q^2 s^2) \Pi(-q^2, k) \\ - (2 - s^2 - 2q^2 s^2) K(k)] \quad (7)$$

and

$$s = \Phi_{0i}/|C| |\Phi_h \Phi_{\bar{h}}|^{1/2}, \quad q = |C| |\text{Im}(\Phi_h \Phi_{\bar{h}})| / \Phi_{0i}, \quad (8)$$

$$k = (1 + s^2 - s^2 q^2)^{-1/2}$$

with

$$\Phi_h = \Phi_{hr} + i\Phi_{hi} \quad (9)$$

and $K(k)$, $E(k)$ and $\Pi(-q^2, k)$ are complete elliptical integrals of the first, second and third type. Clearly, in both the empirical and the analytical approach, the presence of appreciable absorption adds significant complexity to the expression for perfect-crystal reflectivity.

The empirical expression of Hirsch & Ramachandran (1949) (as modified by Cole & Stemple, 1962) agrees with the theoretically rigorous expression of Afans'ev & Perstnev (1969) to within 2% over a wide range of diffraction conditions that are typically encountered in a laboratory setting. Both expressions, however, are rather complicated equations involving many diffraction parameters. In addition, neither expression readily reveals the extent to which the difference between dynamical and kinematic reflectivity depends on the relative strengths of the attenuation mechanisms that characterize the two types of diffraction, namely dynamical extinction and photoelectric absorption. Hirsch & Ramachandran (1949) show that, when the absorption coefficient is much larger than the extinction coefficient, the dynamical integrated reflectivity from a perfect crystal approaches the kinematic reflectivity of an imperfect crystal. The asymptotic approach to the kinematic limit has been described by Wilkins (1978, 1980) in terms of a decrease to zero in the level of interaction between the incident and diffracted waves. This theoretical treatment was a natural extension of the earlier work of Mathieson (1975, 1977) on extinction-free measurements with asymmetric reflections. Wilkins and Mathieson were most interested in examining geometric means for attaining this limit, such as increasing the degree of asymmetry of the Bragg reflection and reducing the thickness of a finite diffracting crystal. In the case of a symmetric reflection from an infinitely thick crystal considered in the present work, this limit can be approached by reducing the structure factor. All three approaches to the zero-level-of-interaction limit are manifested as a reduction in the extinction coefficient relative to the photoelectric absorption coefficient.

As the extinction coefficient becomes larger than the absorption coefficient, the dynamical reflectivity becomes much less than that predicted in the kinematic case and approaches the value predicted by (3). While the determination of structure factors is made most conveniently in the zero-level-of-interaction limit (Wilkins, 1978), an assessment of crystalline perfection should be made within a regime where

strong dynamical interactions are expected. Under these conditions, a significant (or at least measurable) difference between the kinematic and dynamic reflectivities would be anticipated. An examination of the dependence of this difference as a function of the relative magnitudes of the attenuation mechanisms would thus be useful, particularly if it were to yield an expression for the ratio of the dynamic to kinematic reflectivities in terms of parameters that are salient to investigators concerned with characterizing the perfection of single-crystal materials.

The question of how perfect a crystal must be to require the dynamical theory to explain the diffraction process may be addressed by comparing the length over which the crystal has no structural defects (where 'defect' is used to denote a disruption in the periodicity of the lattice) with ξ , the extinction distance from dynamical theory. The extinction distance is the length measured perpendicular to the crystal surface over which the intensity of the wave field is decreased by a factor of $1/e$ due to dynamical interference effects. If the distance between defects in the crystal is less than the extinction distance, dynamical equilibrium cannot be achieved in the crystal and the kinematic theory is sufficient to describe the resulting diffraction. The dynamical expression must be invoked, however, if the crystal is perfect over a length on the order of or greater than the extinction distance. The extinction distance for symmetric Bragg reflections when absorption is negligible is given by (James, 1963)

$$\xi = \pi V_c \sin \theta_B / C \lambda r_e |F_{hkl} F_{\bar{h}\bar{k}\bar{l}}|^{1/2}. \quad (10)$$

The above discussion of the extinction distance suggests that it can be thought of as being inversely proportional to an attenuation coefficient, describing the exponential decay of intensity with depth traversed in the crystal in a manner analogous to the photoelectric absorption coefficient. The difference between the two coefficients lies in the mechanisms by which a decay in intensity occurs. Photoelectric absorption is a loss of energy from the wave field to the atoms of the crystal; this is expressed through μ_n , the effective absorption coefficient normal to the surface in the symmetric Bragg geometry, which in turn can be expressed in terms of the imaginary part of the zeroth Fourier component of the electrical susceptibility, Φ_{0i} :

$$\mu_n = \mu / \sin \theta_B = 2\pi |\Phi_{0i}| / \lambda \sin \theta_B. \quad (11)$$

On the other hand, dynamical extinction is a redistribution of energy within the wave field. Although both absorption and extinction contribute to k_i , the imaginary component of the X-ray's wave vector in the material, they play different roles in determining the intensity of the Bragg reflection due to the different attenuation mechanisms they represent. Both mechanisms are manifested in the complex form of

the Fourier components of the electrical susceptibility. The imaginary contribution representing photoelectric absorption arises from the imaginary components of the individual atomic structure factors, while that representing extinction owes much of its character to geometric factors.

Examination of the above equation for the extinction distance ξ together with (1) and (3) illuminates the role that the two attenuation mechanisms play in determining the ratio of dynamical to kinematic integrated reflection in the limiting case of small absorption. Note that the ratio of (3) to (1) is proportional to the product of the photoelectric absorption coefficient and the extinction distance, $\mu_n \xi$. Consideration of the inverse relationship of ξ and the extinction coefficient shows the above relationship to be nothing more than the physically intuitive statement that the ratio of dynamical to kinematic integrated reflectivity is proportional to the ratio of the attenuation mechanisms that characterize the two types of diffraction. In fact, equations (8) of Hirsch & Ramachandran (1949) and (14) of Afanas'ev & Perstnev (1969) are simple expressions that depend solely on parameters that are proportional to $\mu_n \xi$. This $\mu_n \xi$ dependence is expressed through Hirsch & Ramachandran's variable g in our equation (4) and through Afanas'ev & Perstnev's variable s in our equation (7). These expressions, although simple, are only valid in the limit of small $\mu_n \xi$.

Hence, when absorption is no longer negligible, the more complicated expressions in (4) or (6) above must be invoked to describe the dynamical reflectivity. By parameterizing the ratio of reflectivities in terms of $\mu_n \xi$, we find that a reasonably accurate prediction of the integrated reflectivity over the entire range of $\mu_n \xi$ is obtained without reference to the complex relationship between materials parameters evident in (4) or (7). The starting point for simplifying the above expressions is examining the behavior of the ratio in the limits of large and small $\mu_n \xi$. In the limit of strong absorption and small extinction distance, the reflectivity predicted by the dynamical theory approaches that predicted by the kinematic theory,

$$\lim_{\mu_n \xi \rightarrow \infty} R_{\text{dyn}}/R_{\text{kin}} = 1. \quad (12)$$

When absorption is small in comparison with extinction, the expression for dynamical reflectivity approaches that of James (1963) given above in (3), which leads to the previously mentioned linear dependence of the ratio of reflectivities on $\mu_n \xi$,

$$\lim_{\mu_n \xi \rightarrow 0} R_{\text{dyn}}/R_{\text{kin}} = (16/3\pi^2)\mu_n \xi. \quad (13)$$

In the absorption/extinction regime where (3) is valid, *i.e.* when $\mu_n \xi < 0.3$, the expansion of the exponential function in terms of its linear leading term is accurate within 2%. The behavior of the

relationship in the two limits can then be accounted for within 1% accuracy by the simple function

$$R_{\text{dyn}}/R_{\text{kin}} \approx 1 - \exp [(-16/3\pi^2)\mu_n \xi]. \quad (14)$$

Application of (14) to CdTe

To check the validity of (14), the reflectivities in the dynamical and kinematic limit were calculated for various (111)-type symmetric reflections and wavelengths using (1) and (6). Fig. 1 plots the ratio of dynamical to kinematic reflectivity ($R_{\text{dyn}}/R_{\text{kin}}$) against $\mu_n \xi$ for a series of symmetric (111)-type Bragg reflections from CdTe. The solid line in the figure is generated by (14). The data points in the figure were calculated using the dynamical reflectivity as calculated by use of equation (6) of Afanas'ev & Perstnev (1969). The specific diffraction conditions that were used in the calculation of the reflectivities are tabulated in Table 1. The data in the table were calculated using atomic scattering factors and photoelectric absorption coefficients taken from *International Tables for X-ray Crystallography* (1974) and corrected for temperature using Debye coefficients measured by Horning & Staudenmann (1987). The reflectivity for both σ - ($C = 1$) and π - ($C = \cos 2\theta$) polarized X-rays were calculated in each diffraction condition. The wavelengths considered were those available from the *Bremsstrahlung* spectrum of a typical laboratory X-ray source such as a rotating-anode generator capable of operating at 60 keV with a Cu target. The existence of weak quasiforbidden (111)-type reflections in the sphalerite structures was utilized in conjunction with the different wavelengths to vary the dimensionless quantity $\mu_n \xi$ over two orders of magnitude from 0.03 to 60. Even over this wide range of $\mu_n \xi$ the rather complicated equations yield a physically intuitive relationship between the reflectivities

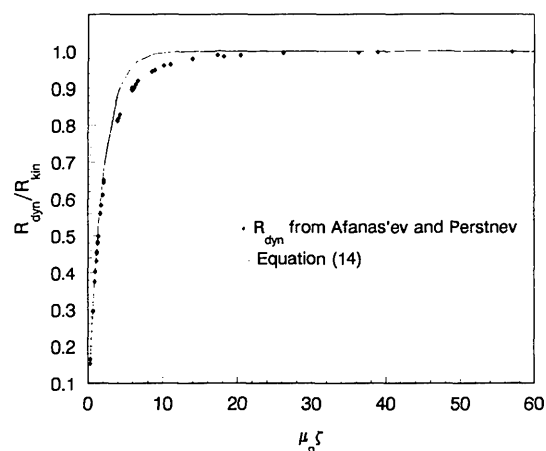


Fig. 1. Comparison of the reflectivity ratios $R_{\text{dyn}}/R_{\text{kin}}$ calculated according to (14) (solid line) with those calculated according to Afanas'ev & Perstnev (1969) (dots).

Table 1. Diffraction conditions corresponding to the calculated data in Fig. 1

$\mu_n \xi$	(hkl)	λ (Å)	C	μ (cm ⁻¹)	ξ (μm)	R_{kin}	R_{dyn}
0.31	(333)	0.51	1.00	72	9.00	4.57E-05	6.93E-06
0.34	(333)	0.51	0.92	72	9.83	3.83E-05	6.28E-06
0.68	(444)	0.77	1.00	232	12.00	2.57E-05	7.59E-06
0.93	(555)	0.62	1.00	126	30.42	5.93E-06	2.26E-06
1.02	(444)	0.77	0.66	232	18.17	1.12E-05	4.52E-06
1.12	(333)	1.03	1.00	618	8.88	2.81E-05	1.18E-05
1.18	(111)	1.54	1.00	1480	1.65	1.99E-04	9.27E-05
1.20	(444)	0.39	1.00	214	11.56	7.08E-06	3.24E-06
1.29	(111)	1.54	0.92	1480	1.80	1.67E-04	8.23E-05
1.31	(444)	0.39	0.92	214	12.64	5.93E-06	2.87E-06
1.41	(555)	0.62	0.66	126	46.05	2.59E-06	1.31E-06
1.69	(333)	1.03	0.66	518	13.45	1.23E-05	6.70E-06
1.81	(555)	0.31	1.00	123	30.29	1.43E-06	8.50E-07
1.98	(555)	0.31	0.92	123	33.10	1.20E-06	7.47E-07
2.11	(444)	1.54	1.00	1480	11.73	2.71E-05	1.77E-05
2.11	(333)	1.54	1.00	1480	8.82	2.60E-05	1.61E-05
3.95	(777)	0.44	1.00	155	105.00	2.88E-07	2.74E-07
3.95	(888)	0.77	1.00	232	140.40	6.04E-07	4.92E-07
4.09	(666)	0.51	1.00	72	233.90	1.45E-07	1.18E-07
4.28	(999)	0.51	1.00	72	367.60	1.02E-07	8.61E-08
5.87	(222)	0.77	1.00	232	52.11	6.35E-07	5.69E-07
5.89	(444)	1.54	0.36	1480	32.77	3.48E-06	3.14E-06
5.98	(777)	0.44	0.66	155	158.90	1.25E-07	1.32E-07
6.19	(666)	0.51	0.66	72	354.10	6.30E-08	5.68E-08
6.41	(222)	0.77	0.92	232	56.95	5.32E-07	4.84E-07
6.71	(888)	0.39	1.00	214	129.20	1.22E-07	1.12E-07
8.57	(666)	0.77	1.00	232	228.40	1.23E-07	1.17E-07
8.94	(333)	1.54	0.24	1480	37.34	1.45E-06	1.32E-06
10.16	(888)	0.39	0.66	214	195.60	5.32E-08	5.11E-08
11.04	(888)	0.77	0.36	232	392.20	7.74E-08	7.47E-08
13.92	(666)	1.03	1.00	518	221.40	1.46E-07	1.43E-07
17.30	(222)	1.54	1.00	1480	48.16	5.00E-07	4.95E-07
18.14	(999)	0.51	0.24	72	1557.00	5.70E-09	5.70E-09
20.41	(10,10,10)	0.62	1.00	126	1335.00	9.91E-09	9.80E-09
26.20	(222)	1.54	0.66	1480	72.92	2.18E-07	2.17E-07
36.30	(666)	0.77	0.24	232	967.00	6.88E-09	6.86E-09
38.87	(666)	1.03	0.36	518	618.40	1.87E-08	1.86E-08
57.00	(10,10,10)	0.62	0.36	126	3728.0	1.27E-09	1.27E-09

and the parameter that describes the relative strength of their attenuation mechanisms.

Although (14) was derived only by considering the limits of the diffracting behavior without reference to any materials constants except $\mu_n \xi$, it predicts the reflectivity with an error of no greater than 9% in the cases considered. The difference between the two expressions is plotted against $\mu_n \xi$ in Fig. 2. The

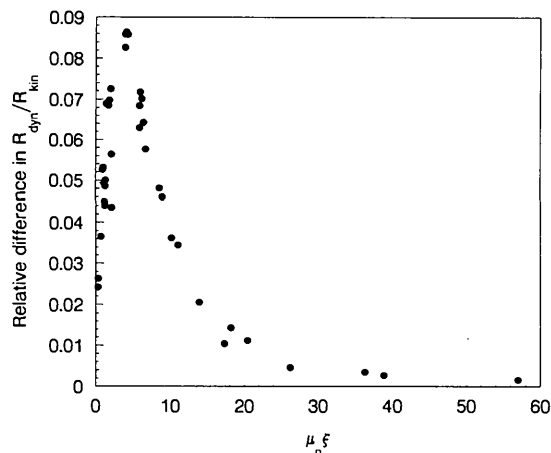


Fig. 2. Relative difference between the reflectivity ratios illustrated in Fig. 1.

approximation is considerably better than 9% in the limits of large and small $\mu_n \xi$ and, for many purposes, the accuracy in the intermediate regime may be acceptable in light of the relationship's computational expediency and physical intuitiveness. Note that this difference varies systematically with $\mu_n \xi$, suggesting that additional refinement would yield even better agreement with the rigorous theoretical treatment of Afanas'ev & Perstnev (1969). However, there is no need for a more accurate interpolation formula than that which already exists. The present relationship is intended rather to illustrate the strength of the dependence of the reflectivity ratio on the ratio of attenuation coefficients.

A natural extension of this work would be to consider different families of reflections (*i.e.* $\langle 100 \rangle$ - and $\langle 110 \rangle$ -type Bragg reflections) and different materials systems in the examination of the functional form of the differences plotted in Fig. 2. Since diffraction geometries were not drawn upon in deriving (14), it is not expected that the relationship would change in a qualitative sense. Investigations of these types would rather serve as a useful framework in which to understand the physical source of those refinements whose need is indicated by Fig. 2.

Discussion

The accuracy of the above expression in predicting the dynamical reflectivity of the crystal is remarkable when the gross simplifications that were made in (14) are taken into consideration. Indeed, the complicated form of the expressions of Hirsch & Ramachandran (1949) or Afanas'ev & Perstnev (1969) are necessary if a higher degree of accuracy is required. The relative success of an expression such as the one presented here effectively exhibits the overwhelming dependence of the reflectivity ratio on $\mu_n \xi$ as compared to the other parameters in the former equations.

The usefulness of a simple relation such as that in (14) to the experimentalist who wishes to gauge the perfection of crystalline materials by reflectivity measurements deserves further discussion. For example, the full width at half-maximum (FWHM) of a double-crystal X-ray rocking curve is a figure of merit used to assess the perfection of a crystal. Inspection of the relationship derived above in (14) suggests an avenue to address two major concerns in this method of characterizing defective single crystals: (1) how sensitive are the diffraction conditions to crystalline imperfection and (2) is the broadening of the peak due to the presence of a statistical distribution of defects dense enough to make the crystal behave kinematically or is it due to the presence of large dynamically diffracting perfect regions in the crystal that are slightly misoriented with respect to each other?

The first question is addressed by calculating the product $\mu_n \xi$ for the material under a certain set of diffraction conditions. Note that in Fig. 1 the ratio of dynamical to kinematic integrated reflectivity approaches unit for large $\mu_n \xi$: the larger the product, the less sensitive the measurement is to crystalline imperfection. Although it is the integrated reflection and not the shape of the peak that is the dependent quantity in this study, the crystallographer would be prudent in choosing diffraction conditions with as small a $\mu_n \xi$ as is practical when assessing the material's perfection with X-ray rocking curves.

The second concern is addressed by measuring the integrated reflectivity of the rocking curve as well as its shape. If the crystal consists of large (with respect to the extinction distance) perfect regions, the integrated intensity will be that predicted by the dynamical theory instead of the kinematic theory. Although Zachariassen's (1967) treatment of integrated reflectivity from defective crystals in principle allows a more detailed analysis, it presupposes that the angular misorientations of perfect-crystal regions can be described by a Gaussian distribution and that absorption effects are not large. It has been shown that many materials do not exhibit a Gaussian distribution of misorientations of perfect-crystal regions (Schneider, 1980). In addition, in a highly absorbing material such as CdTe, it is quite possible that under normal laboratory experimental conditions the assumption of small absorption effects may also be incorrect. In a set of experiments published elsewhere (Moran & Matyi, 1991), the authors study two crystals of CdTe with etch-pit densities differing by two orders of magnitude. Both had approximately the same integrated reflectivity (indicative of dynamical diffraction); however, the FWHM of double-crystal rocking curves from the two CdTe samples were significantly different. The explanation for this behavior, that defects were in both cases confined to boundaries between large structurally perfect regions, was confirmed *via* X-ray topography. The integrated reflectivity, interpreted within the framework of the above relation, was thus found to be a useful quantity

for understanding the shape of the rocking curve in terms of the sample's defect structure.

Concluding remarks

A relationship between the ratio of dynamical to kinematic integrated reflectivity and the product of two salient diffraction parameters, the photoelectric absorption coefficient and the extinction distance, has been developed. This relationship is a computationally expedient approximation to the theoretically rigorous expression derived by Afanas'ev & Perstnev (1969). In the specific case of $\langle 111 \rangle$ CdTe, the approximation has been shown to agree to within 9% over a wide range of diffraction conditions. The success of this simple approximation arises from the strong dependence of the ratio of dynamic to kinematic reflectivities on the relative strengths of the attenuation mechanisms that characterize each diffraction process.

This work was supported in part by National Science Foundation Grant no. DMR-8907372.

References

- AFANAS'EV, A. M. & PERSTNEV, J. P. (1969). *Acta Cryst.* **A25**, 520-523.
- COLE, H. & STEMPEL, N. R. (1962). *J. Appl. Phys.* **33**, 2227-2233.
- HIRSCH, P. B. & RAMACHANDRAN, G. N. (1949). *Acta Cryst.* **3**, 187-194.
- HORNING, R. D. & STAUDENMANN, J.-L. (1987). *Phys. Rev. B*, **36**, 2873-2874.
- International Tables for X-ray Crystallography* (1974). Vol. IV. Birmingham: Kynoch Press. (Present distributor Kluwer Academic Publishers, Dordrecht.)
- JAMES, R. W. (1963). *Solid State Phys.* **15**, 53-220.
- MATHIESON, A. MCL. (1975). *Acta Cryst.* **A31**, 769-774.
- MATHIESON, A. MCL. (1977). *Acta Cryst.* **A33**, 610-617.
- MORAN, P. D. & MATYI, R. J. (1992). *J. Appl. Cryst.* **25**, 358-365.
- SCHNEIDER, J. R. (1980). *Characterization of Crystal Growth Defects by X-ray Methods*, edited by B. K. TANNER & D. K. BOWEN, pp. 186-215. New York: Plenum.
- WHITE, J. E. (1950). *J. Appl. Phys.* **23**, 855-859.
- WILKINS, S. W. (1978). *Proc. R. Soc. London Ser. A*, **364**, 569-589.
- WILKINS, S. W. (1980). *Acta Cryst.* **A36**, 143-146.
- ZACHARIASEN, W. H. (1967). *Acta Cryst.* **23**, 558-564.